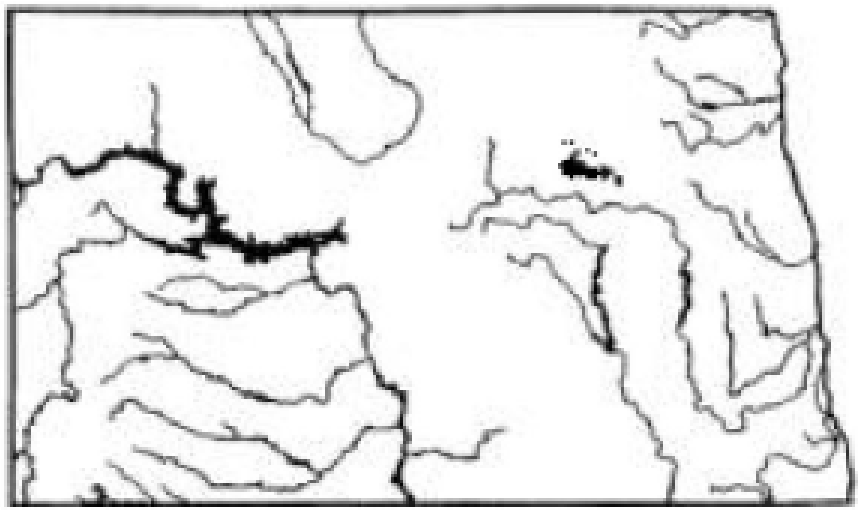

Technical Report No: ND13-03

EFFECTIVE DELIVERY OF IRON NANOPARTICLES BY AMPHIPHILIC POLYSILOXANE GRAFT COPOLYMERIC VEHICLES FOR GROUNDWATER REMEDIATION

by
Sita Krajangpan
Bret J. Chishlom
Achintya N. Bezbaruah

Dept. of Civil Engineering
North Dakota State University
Fargo, North Dakota

June 2013

North Dakota Water Resources Research Institute
North Dakota State University, Fargo, North Dakota

Technical Report No: ND13-03

EFFECTIVE DELIVERY OF IRON NANOPARTICLES BY AMPHIPHILIC POLYSILOXANE GRAFT COPOLYMERIC VEHICLES FOR GROUNDWATER REMEDIATION

by
Sita Krajangpan[1]
Bret J. Chisholm[2]
Achintya N. Bezbaruah[3]

WRRI Graduate Research Fellow[1]
Senior Research Scientist, Center for Nanoscale Science and Engineering[2]
Professor, Department of Civil Engineering[3]
North Dakota State University
Fargo, ND 58108

June 2013

The work upon which this report is based was supported in part by federal funds provided by the United States of Department of Interior in the form of ND WRRI Graduate Research Fellowship for the graduate student through the North Dakota Water Resources Research Institute.

Contents of this report do not necessarily reflect the views and policies of the US Department of Interior, nor does mention of trade names or commercial products constitute their endorsement or recommendation for use by the US government.

Project Period: March 1, 2007 – February 28, 2009
Project Numbers: 2007ND150B, 2008ND 164B, and 2009ND184B

North Dakota Water Resources Research Institute
Director: G. Padmanabhan

North Dakota State University
Fargo, North Dakota, 58108

TABLE OF CONTENTS

LIST OF TABLES……...v

LIST OF FIGURES…….v

ABSTRACT…….1

ACKNOWLEDGMENTS……...2

BACKGROUND…….3

DESCRIPTION OF THE CRITICAL STATE OR REGIONAL WATER

PROBLEM INVESTIGATED…….4

SCOPE AND OBJECTIVES……...4

MATERIALS AND METHODS…….5

NZVI synthesis and characterization…….5

APGC synthesis and characterization……5

CNZVI preparation and characterization.……..……...8

Colloidal stability studies.....8

Effect of ionic strength on colloidal stability of CNZVI.....8

Effect of aging on colloidal stability of CNZVI.....8

TCE degradation batch studies.....8

Effect of aging on TCE degradation by CNZVI.....9

Arsenic removal batch studies.....9

Effect of ionic strength on As(V) removal.....9

Quality control and statistical analysis.....10

RESULTS AND DISCUSSION……...10

NZVI synthesis and characterization……...10

APGC synthesis and characterization……..10

CNZVI preparation…….…….15

Colloidal stability studies.....16

Effect of ionic strength on colloidal stability of CNZVI 17

Effect of aging on colloidal stability of CNZVI.....18

TCE degradation batch studies.....18

Effect of aging on TCE degradation by CNZVI.....21

As(V) removal batch studies.....23

Effect of ionic strength on As(V) removal.....26

CONCLUSIONS……..26

REFERENCES……..27

LIST OF TABLES

Table 1. Weight fractions of the three different repeat units of APGC used to optimize the APGC composition.....7

Table 2. The characteristics of the synthesized NZVI and the commercial grade MZVI.....12

Table 3. Peak assignments and wave numbers for FTIR spectra of polymer before hydrolysis (PDMS/PEG/tBA), polymer after hydrolysis (PDMS/PEG/AA), and CNZVI…….14

Table 4. Summary of TCE degradation reaction rate constants with bare NZVI and CNZVI.....22

Table 5. Summary of arsenic removal rate constants with bare NZVI and CNZVI.....24

LIST OF FIGURES

Figure 1. The APGC synthesis process……..……..6

Figure 2. TEM images of bare NZVI…….11

Figure 3. Particle size distribution of NZVI……..11

Figure 4. XRD spectrum of synthesized iron NPs showed only Fe^0 ……12

Figure 5. ^1H NMR of the final product (APGC)……13

Figure 6. ^{13}C NMR spectrum of APGC (after hydrolysis).....13

Figure 7. (a) FT-IR spectrum of APGC before hydrolysis; (b) FT-IR spectrum after hydrolysis; (c) FT-IR spectrum of CNZVI……...14

Figure 8. Differential scanning calorimetry (DSC) thermogram of APGC……...……15

Figure 9. The APGC with the highest acrylic acid group (PDMS/PEG/AA (72.5/21/6.5)) showed the highest colloidal stability…….16

Figure 10. Sedimentation studies of CNZVI in water with different ionic strengths……17

Figure 11. Sedimentation studies for CNZVI over a 12-month period for shelf-life evaluation..18

Figure 12. Dechlorination of TCE by bare NZVI and CNZVI. Initial TCE concentration = 30 mg/L……..19

Figure 13. Dechlorination of TCE by bare NZVI and CNZVI. Initial TCE concentration = 15 mg/L……..20

Figure 14. Dechlorination of TCE by bare NZVI and CNZVI. Initial TCE concentration = 1 mg/L……..20

Figure 15. TCE degradation studies using CNZVI over a 6-month period (shelf-life evaluation)…….22

Figure 16. As(V) removal over time (initial As(V) concentration is 10 mg/L)…….....24

Figure 17. As(V) removal over time (initial As(V) concentration is 5 mg/L)……...25

Figure 18. As(V) removal over time (initial As(V) concentration is 1 mg/L)……...25

Figure 19. Effects of ionic strength on arsenic removal by CNZVI under aerobic conditions….26

ABSTRACT

Nanoscale zero-valent iron (NZVI) particles have been surface modified and used for contaminant remediation. NZVI tend to agglomerate due to magnetic and van der Waals forces and form larger particles that settle down in aqeous media. NZVI particles are used for contaminant remediation and the remediation process is known to be surface area mediated. Agglomeration increases particle size and decrease specific surface area which leads to decrease in their reactivity. A novel amphiphilic polysiloxane graft copolymer (APGC) was designed, synthesized and used to coat NZVI to overcome the agglomeration problem. APGC was composed of hydrophobic polysiloxane, hydrophilic polyethylene glycol **(**PEG), and carboxylic acid. The APGC was successfully adsorbed onto the NZVI surfaces via the carboxylic acid anchoring groups and PEG grafts provided dispersibility in water. The APGC possessing the highest concentration of carboxylic acid anchoring group provided the highest colloidal stability. It was also found that the colloidal stability of the APGC coated NZVI remained effectively unchanged up to 12 months. The sedimentation characteristics of APGC coated NZVI (CNZVI) under different ionic strength conditions (0-10 mM NaCl and $CaCl_2$) did not change significantly. Degradation studies were conducted with trichloroethylene (TCE) and arsenic [As(V)] as the model contaminants. TCE degradation rates with CNZVI were determined to be higher as compared to bare NZVI. Shelf-life studies indicated no change in TCE degradation behavior by CNZVI over a 6-month period. As(V) removal batch studies with CNZVI were conducted in both aerobic and anaerobic conditions. Increase in arsenic removal efficiency was observed with CNZVI as compared to bare NZVI in both aerobic and anaerobic conditions. Ionic strengths showed minimal (4-8%) inhibiting effect on arsenic removal by CNZVI.

ACKNOWLEDGEMENTS

Stipend support to Krajangpan and supplemental funding from the North Dakota Water Resources Research Institute are thankfully acknowledged. North Dakota State University (NDSU) Development Foundation, Department of Civil Engineering, and NDSU's Center for Nanoscale Science and Engineering also provided support for this work. Part of this work was supported by a grant from National Science Foundation (PI: Bezbaruah, Grant#CMMI-1125674).

BACKGROUND

Zero-valent iron (ZVI) is known to remediate and number of contaminants and reactions are known to be surface mediated (Matheson and Tratnyek, 1994; Li et al., 2006). Hence, higher specific surface area (i.e. surface area per unit mass) of ZVI is expected to lead to higher degradation of contaminants. While conventionally used microscale zero-valent iron (MZVI) has very low specific surface area of 1-2 m^2/g (Thompson et al., 2010), nanoscale zero-valent iron (NZVI) has a surface area of 25-54 m^2/g (Chen et al., 2004; Li et al., 2006; Bezbaruah et al., 2009). The NZVI with higher reactive surface area are expected to work better for contaminant remediation and these nanoparticles react with contaminant approximately 1,000 times faster than micro scaled zero-valent iron (MZVI) (Kanel et al., 2005; Kanel et al., 2006). In addition to having higher reactive surface area, NZVI have other unique physico-chemical properties such as smaller size (<100 nm) and higher interparticle interactions and magnetic properties. NZVI have been used for the removal of various groundwater contaminants including chlorinated compounds (Liu and Lowry, 2006; Cheng et al., 2007; Katsenovich and Miralles-Wilhelm, 2009, Bezbaruah et al., 2011, Krajangpan et al., 2012), pesticides (Feitz et al., 2005; Joo et al., 2008; Thompson et al., 2010), heavy metals (Xi et al., 2010; Klimkova et al., 2011), non-metallic inorganics (Bezbaruah et al., 2009, Almeelbi and Bezbaruah, 2012) and explosives (Zhang et al., 2010).

While NZVI particles have been used for groundwater remediation, they tend to agglomerate due to magnetic and van der Waals forces, and form larger particles that settle into aquifer media pores. Agglomerated particles have decreased specific surface area. As NZVI based reactions are surface mediated, the loss of specific surface area leads to decrease in reactivity of NZVI (Krajangpan et al., 2008; Tiraferri et al., 2008; Bezbaruah et al., et al., 2009; Krajangpan et al., 2012). To overcome these problems, it is necessary to ensure that each NZVI particle can disperse independently and the particles have reduced interparticle attractions. Further, NZVI particles should be easily injectable to the aquifer matrix for groundwater contaminant remediation. Injecting NZVI into the aquifer is considered a standard practice for groundwater remediation. However, NZVI particles have a high sticking coefficient and they get attached to aquifer materials (Saleh et al., 2007). Subsurface mobility of nanoscale iron is limited by particle-soil grain attachment and particle-particle agglomeration (Quinn et al., 2005; Saleh et al., 2007; Phenrat et al, 2009; Krajangpan et al., 2012). It has been demonstrated that nanoparticles dispersibility is quite limited without appropriate particle surface modification (Saleh et al., 2007; Krajangpan et al., 2008; Krajangpan et al., 2012). It is, therefore, necessary that the NZVI particles be surface modified to achieve proper dispersion.

In this study, graft copolymers were designed for surface modification of NZVI particles which in turn was expected to resist NZVI agglomeration and sedimentation in aqueous solution. The new graft copolymers consisted of a polysiloxane backbone, polyethylene glycol grafts, and pendent carboxylic acids as anchoring groups. It was hypothesized that a polysiloxane polymer backbone possessing pendent carboxylic acid would enable efficient adsorption of the polymer to NZVI surfaces because of the affinity of carboxylic acid groups for iron and the low surface tension of polysiloxanes. The water-soluble PEG grafts would serve to provide dispersibility and colloidal stability of coated particles in the aqueous media. The polysiloxane, being non-polar

and possessing a very low glass-transition temperature, was expected to readily allow permeation of contaminants through it onto NZVI surfaces.

Degradation studies were conducted with trichloroethylene (TCE, C_2HCl_3) and arsenic(V) [As(V)] as the model contaminants. TCE represents one of the most problematic classes of volatile organic compounds found in contaminated groundwater (Wu and Schaum, 2000). A number of studies have demonstrated that the widespread presence of TCE in groundwater is a serious public health concern due to the hazardous nature of this contaminant (Ellis and Rivett, 2007; Pant and Pant, 2010; Tsai et al., 2011). Arsenic is considered a potential carcinogen to human (Lisabeth et al., 2010). Increased concentrations of arsenic in natural water have been reported in many areas all over the world including South East Asia (Bangladesh, Vietnam, India, Nepal, Cambodia, Mongolia, China, Thailand, Pakistan and Taiwan), Central and South America (Mexico, Chile and Argentina), North America (USA and Canada), and Australia (Berg et al., 2001; Kanel et al., 2006; Hussam and Munir, 2007).

DESCRIPTION OF THE CRITICAL STATE OR REGIONAL WATER PROBLEM INVESTIGATED

Arsenic contamination is a major concern in southeast North Dakota (568 sq mile area in Sargent, Ransom and Richland counties are affected). The contaminated area is primarily comprised of farmland and a few small cites including Hankinson, Lindrud, Wyndmere, and Milnor. Sampling done since 1979 in that area indicated arsenic concentration as high as 1.5 mg/L as against the United States Environmental Protection Agency's stipulated drinking maximum contaminant level (MCL) of 10 µg/L. The contamination of arsenic is not only a major concern in North Dakota but also in many states of the USA. For example, arsenic concentrations have been found to be 1-11,330, 1-2,240, 50-2,500,000, 3-110, and >50 µg/L in Massachusetts, Maryland, Texas, South Dakota and North Dakota, respectively.

In addition, there are concerns about the TCE at West Fargo and Minot in North Dakota and at the Baytown Ground Water Contamination Site in Washington County, Minnesota. The stakeholders have looked at NZVI as a potential remedy for source zone and at-well applications. The surface modified NZVI to be designed within this project would find applications in remediation of such and similar contaminants. With the surface modified NZVI synthesized in this research, effective remediation of arsenic in groundwater would be achieved and that would provide protection to public health in North Dakota.

SCOPE AND OBJECTIVES

The broad objective of this study was to modify NZVI particles using polymers to achieve better dispersibility and less agglomeration for application in groundwater remediation.

The specific objectives of the study were as follows:

1) Design a new polymeric surface modifier for NZVI to achieve increased dispersibility of the particles;

2) Fine tune the design of the coated (modified) NZVI (CNZVI) for effective degradation of TCE and As(V);
3) Determination of longevity (shelf-life) of CNZVI; and
4) Determine whether ionic strength effects colloidal stability and contaminant degradation by CNZVI.

MATERIALS AND METHODS

Iron(II) sulfate heptahydrate ($FeSO_4 \cdot 7H_2O$, 99%, Alfa Aesar), sodium borohydride ($NaBH_4$, 98%, Aldrich), iron powder (<10 μm, 99.9%, Aldrich), calcium chloride ($CaCl_2$, ACS grade, BDH), sodium alginate (production grade, Pfaltz & Bauer), methanol (production grade, BDH), and ethanol (ACS grade, Mallinckrodt Chemicals) were purchased from VWR (West Chester, PA) and were used as received unless otherwise specified. Dichloromethane (purity 98%), PtO_2 (99.5+%), *tert*-butyl acrylate, toluene (HPLC grade), and trifluoroacetic acid (99.5%) were all obtained from Aldrich Chemical and used as received. Sodium hydroxide (NaOH, ACS grade, BDH), sodium chloride (NaCl, 99%, Fisher Scientific), Poly(methylhydrosiloxane-dimethylsiloxane) (HMS-151, Gelest), polyethylene glycol allylmethyl ether (polyglykol AM 350, Clariant), and He and N_2 (both from Praxair) and all other chemicals were used as received unless otherwise specified.

NZVI synthesis and characterization

Iron nanoparticles were synthesized by borohydride reduction of ferrous ion in $FeSO_4.7H_2O$ in an aqueous phase (Lui et al., 2006; Bezbaruah et al., 2009; Bezbaruah et al., 2011). The use of this method is well documented (Li et al., 2006). The method is inexpensive and requires no specialized equipment. Additionally, the nanoparticles synthesized by this method have shown both high reactivity and durability (Lui et al., 2006). The reaction scheme for the synthesis is as follows:

$$2\ Fe^{2+} + BH_4^- + 3H_2O \rightarrow 2Fe^0\downarrow + H_2BO_3^- + 4H^+ + 2H_2 \quad (1)$$

The NZVI obtained was dried in a vacuum oven for ~6 h and allowed to stand at ambient conditions overnight to passivate the iron (Bezbaruah et al., 2009; Bezbaruah et al., 2011). Similar passivation techniques were employed by Sohn et al. (2006) for increased stability of NZVI. The dried NZVI was ground in a ceramic mortar and pestle and stored in a dry nitrogen atmosphere. Transmission electron microscopy (TEM, JEOL JEM-100CX II) images were used to determine particle size distribution. Scanning electron microscopy along with energy dispersive spectroscopy (SEM/EDS, JEOL JSM-6300) was used to observe surface morphology and characterize the elemental composition of NZVI. X-ray diffraction (XRD) was used to identify the chemical composition of the NZVI.

APGC synthesis and characterization

APGCs were synthesized using a three-step process (Figure 1). In Step 1, 10 g of poly(methylhydrosiloxane-dimethylsiloxane) (PDMS, MW 1950, 20.4 mmol hydride) and 3.57 g polyethylene glycol allylmethyl ethers (PEG, MW 350, 10.2 mmol) were dissolved in 30 mL

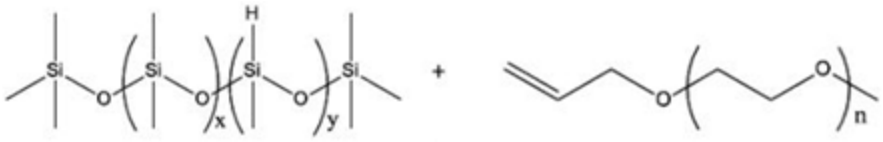

Poly(dimethylsiloxane)

Step 1 **Hydrosilylation**

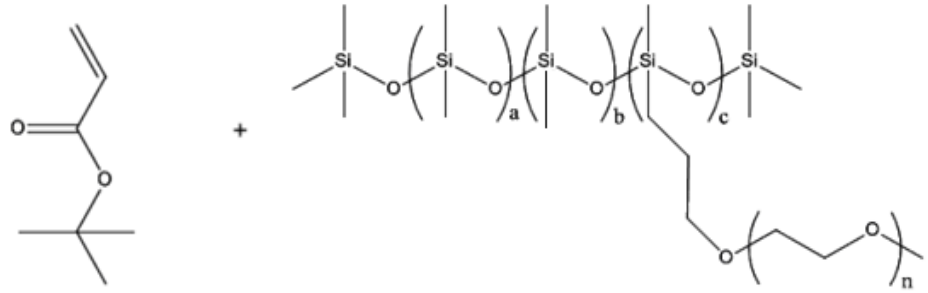

tert-Butnyl acrylate Copolymers of PDMS and PEG

Step 2 **Hydrosilylation**

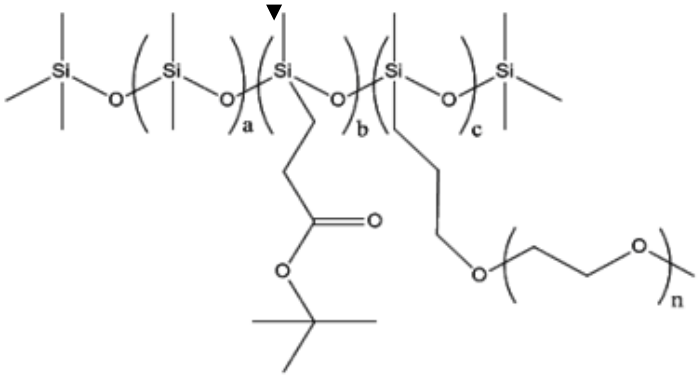

Copolymers with pre-anchoring group

Step 3 **Hydrolysis**

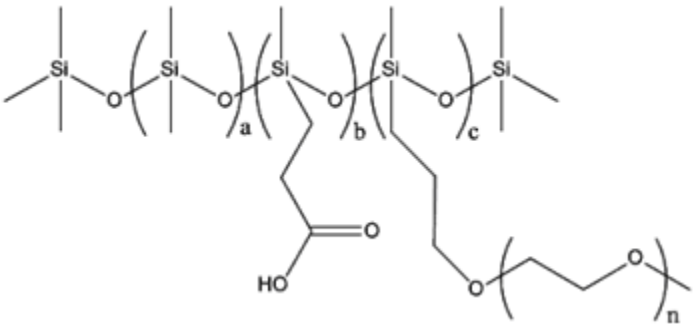

Amphiphilic polysiloxane graft copolymer

Figure 1. The APGC synthesis process (Nationalized PCT Patent, Bezbaruah et al., 2011).

toluene. A catalytic amount of PtO_2 was added, and the mixture heated at 90°C for ~5 h (Sabourault et al., 2002). Upon completion of the hydrosilylation reaction (confirmed through proton nuclear magnetic resonance (^{1}H NMR) spectroscopy (JEOL ECA 400 MHz, JOEL Ltd.)), 1.31 g *tert*-butylacrylate (tBA, MW 128.17, 10.2 mmol) was added to the product and heated at 90°C for ~5 h (Step 2). Upon completion of the second hydrosilylation reaction, the reaction mixture was cooled to room temperature (22±2^{o}C). Platinum oxide was removed by filtration through a series of $NaHCO_3$ columns, and the copolymer (PDMS/PEG/tBA) was isolated by vacuum stripping the toluene. Step 3 was performed to generate the carboxylic acid (AA) anchoring groups by hydrolyzing the *tert*-butyl ester groups of the graft copolymers. The PDMS/PEG/tBA (10 g of the product synthesized in Step 2) was dissolved in 25 mL of dichloromethane in a 100 mL round bottom flask. Trifluoroacetic acid (TFA, 2.52 mL) was added to the solution, and the mixture was stirred for ~6 h at room temperature to complete the reaction.

The synthesized APGC was isolated by vacuum stripping the dichloromethane, TFA, and *tert*-butanol (a tBA hydrolysis product). Carbon nuclear magnetic resonance (^{13}C NMR, JEOL ECA 400 MHz, JOEL Ltd.) spectroscopy and Fourier transform infrared (FTIR, Nicolet 8700, Thermo Scientific) spectroscopy were used to confirm the completion of hydrolysis. The APGC was either immediately used to coat NZVI or stored in a refrigerator (4^{o}C) by dissolving it in toluene. The stored APGC was used to coat NZVI after evaporating toluene by passing N_2 gas through the solution. The complete removal of toluene was checked using ^{1}H NMR. Five different APGCs were synthesized each varying from the other in terms of the content (weight fraction) of the three different repeat units (Table 1). Glass transition temperature (T_g) of the APGC was measured using differential scanning calorimetry (DSC, DSC Q 1000, TA Instruments Inc.).

Table 1. Weight fractions of the three different repeat units of APGC used to optimize the APGC composition

Sample*	**% Weight fractions**		
	PDMS	**PEG**	**AA**
70/25/5	70	25	5
62/36/2	62	36	2
72.5/21/6.5	72.5	21	6.5
67/29/4	67	29	4
65/32/3	65	32	3

APGC concentration used was 15 g/L

*Weight fraction was decided based on mole fraction needed for reactions to take place

CNZVI preparation and characterization

NZVI particles (60 mg) were combined with 20 mL of APGC of various concentrations (2, 10, and 15 g/L APGC in deoxygenated deionized water or DDW). The mixtures were sonicated for 30 min to disperse the NZVI and rotated in a custom-made end-over-end shaker (28 rpm) for 72 h to allow the APGC to adsorb (i.e. coat) onto the NZVI surface. The CNZVI suspension was stored in borosilicate glass bottles at room temperature. FTIR spectra were obtained with a Nicolet 6700 FTIR Spectrometer operated with OMNIC software. The spectra

were obtained from 400 to 4000 cm^{-1}. The solid samples (NZVI and CNZVI) were dried in a vacuum oven for two days before analysis. The dried samples were then mixed with KBr corresponding to an approximate mass ratio of 1:10 (sample: KBr) for pellet preparation. The liquid samples (PDMS/PEG/tBA and APGC) were prepared by adding the samples as droplets to KBr pellet. The spectra were recorded at a resolution of 4 cm^{-1} with each spectrum corresponding to the co-addition of 64 scans. The background collected from KBr was automatically subtracted from the sample spectra. Bright field images of CNZVI were obtained by using high-resolution transmission electron microscopy (HRTEM) (JEOL JEM-2100 LaB_6, JOEL Ltd.) attached with GATAN Orius SC1000 CCD camera.

Colloidal stability studies

The colloidal stability of the CNZVI was evaluated by measuring sedimentation rates of CNZVI suspensions. A 20 mL suspension of CNZVI (3 g/L of NZVI) in a 20 mL vial was centrifuged (1800 rpm, Heraeus Labofuge 400R Centrifuge, Thermo Electron Corporation) and washed three times with copious amounts of DDW to remove any excess non-adsorbed APGC. Fresh DDW (20 mL) was added to the CNZVI The mixture in the vial was shaken well, and 2 mL of CNZVI suspension in water was withdrawn to a glass cuvette. The sedimentation behavior of the CNZVI was interpreted from the change of light intensity at the wave length of 508 nm over time (2 h) using a UV spectrophotometer (Cary 5000, Varian). The same evaluation was done for a control using 3 g/L bare NZVI in DDW and following the same procedure as in the case CNZVI.

Effect of ionic strength on colloidal stability of CNZVI

This study was conducted with mono-valent (5 and 10 mM NaCl) and divalent cationic (5 and 10 mM $CaCl_2$) salts in 20 mL borosilicate glass vials. CNZVI (3 g/L of NZVI) was added to 20 mL of the doxygenated ionic water. The colloidal stability of the particles in the ionic solution was determined using the same method decribes earlier (see ‘Colloidal stability studies‘).

Effect of aging on CNZVI colloidal stability

Many 20 mL vials of CNZVI (60 mg of NZVI per each batch i.e., 3 g/L NZVI) were prepared and stored in a cabinet at room temperature and their colloidal stability investigated every month over a 12-month period. Three sacrificial vials were taken out of the cabinet every month and their colloidal stability was measure as per method described earlier (see ‘Colloidal stability studies‘). The results were reported as average of the three values along the standard deviations.

TCE degradation batch studies

Batch experiments were conducted in 20 mL amber glass bottles fitted with Teflon septa stoppers. TCE (1, 15, and 30 mg/L initial concentrations) was used as the test contaminant. TCE solutions were prepared with DDW. Bare NZVI (1.5 g/L) or CNZVI (1.5 g/L of NZVI) were added into 20 mL TCE solution. Controls with only APGC (no NZVI) in TCE solution and blank

with only TCE solution were run and analyzed simultaneously following the same procedure used for bare NZVI and CNZVI batch studies. The reactors were rotated end-over-end at 28 rpm in a custom-made shaker to reduce mass transfer resistance. Aliquots were withdrawn from sacrificial batch reactors at pre-determined time intervals (0, 30, 60, 120, 180, and 360 min) and filtered using a syringe filter (Whatman ANOTOP 25, 0.02 µm) to remove NZVI and CNZVI before analyzing using GC/MS (Model 5975, Agilent). The temperatures for GC/MS analyses were as follows: column, injector 200°C, and detector 360°C. Helium was used as the carrier gas at 30 mL/min. Samples were heated at 110°C in an autosampler chamber for 30 min before being vented into the GC. Each sample was run for 8 min. The detection limit of the GC/MS for TCE was 1 µg/L.

Effect of aging on TCE degradation by CNZVI

Several 20 mL vials of CNZVI (60 mg of NZVI per each batch i.e., 3 g/L NZVI) were prepared and stored in a cabinet at room temperature and investigated every month over a 6-month period for the treatability of TCE. Three sacrificial vials were taken out of the cabinet every month and TCE degradation studies were conducted as per method described earlier (see 'TCE degradation batch studies'). The results were reported as average of the three values along the standard deviations.

Arsenic removal batch studies

Arsenic removal batch studies were performed under anaerobic and aerobic conditions in 40 mL commercial grade borosilicate glass reactors with silicone septum cap. A 100 mg/L As(V) stock solution was prepared using As_2O_5 and used to make the initial As(V) concentrations of 1, 5, and 10 mg/L. Bare NZVI and CNZVI (0.75 g/L NZVI concentration for both) were used in a 40 mL As(V) solution. Controls with APGC in the As(V) solution and blanks with only the As(V) solution were run simultaneously. All experiments were conducted in triplicate. To simulate anaerobic conditions the As solutions in reactors were purged with N_2 gas. To reduce mass transfer resistance, the reactors were rotated end-over-end at 28 rpm in a custom-made shaker. Aliquots were withdrawn at definite time intervals and filtered using a syringe filter (Whatman ANOTOP 25, 0.02 µm) to remove NZVI and CNZVI. Samples were preserved using nitric acid for As analysis using an inductively coupled plasma (ICP) spectrophotometer. A Spectro Genesis ICP-OES (Crossflow nebulizer, SOP) was used to analyze As(V) concentration in test solutions. The software used for this analysis was SmartAnalyzer (version v. 3.013.0752). The plasma power, coolant flow, auxiliary flow, nebulizer flow were optimized to 1400, 13.5, 1.2, and 1.0 L/min, respectively, for this instrument. Five-point calibration was performed before testing. The arsenic standard and sample solutions were prepared in 5% HNO_3. The measurement time was 24 sec and pre-flush time was 60 sec. The results were mean concentrations (mg/L) of three replicate measurements along with standard deviations.

Effect of ionic strength on As(V) removal

This study was conducted with 10 mM of NaCl and $CaCl_2$ under aerobic conditions in 40 mL reactors made of commercial grade borosilicate glass vials fitted with silicone septum cap . The initial As(V) concentration was 10 mg/L. The CNZVI concentration was the same as that

used for arsenic removal batch studies (0.75 g/L NZVI) described earlier (see Arsenic removal batch studies). Blanks were run with only As(V) solution. Controls with CNZVI and As(V) solution but without any $NaCl/CaCl_2$ were run simultaneously.

Quality control and statistical analysis

All experiments were conducted in triplicates and average values reported along with standard deviations. Two-way ANOVA analysis was used to find statistical significance while comparing the results.

RESULTS AND DISCUSSION

NZVI synthesis and characterization

Analysis of TEM images (example in Figure 2) indicates that NZVI particle size ranged from 10 to 90 nm with an average size of 35 nm (Figure 3). NZVI particles are seen as clusters (Figure 2). The particles were agglomerated because of strong magnetic interaction between them. This agglomeration limits the availability of reactive surface area on the particle (Schlicker et al., 2003; Bezbaruah et al., 2009; Krajangpan et al., 2012).

A higher magnification TEM image showed a ~2.5 nm of passivating oxide shell around the NZVI core (inset of Figure 2). An oxide shell, possibly of amorphous FeOOH(Cao et al., 2008; Martin et al., 2008), is clearly visible around the nanoparticles. The shell was formed during the passivation process of NZVI. Similar NZVI core/shell geometry was reported earlier by Nurmi et al. (2005) and Li et al. (2006). The oxide shell protects the particles from rapid oxidation, yet allows contaminants access to NZVI surface (Li et al., 2006). XRD spectrum showed only Fe^0 in the synthesized NZVI (Figure 4). TEM, BET, and SEM/EDX results of NZVI compared with micro-sized zero-valent iron (MZVI) are summarized in Table 2.

APGC synthesis and characterization

APGC was synthesized successfully within this research. The progress of reaction during the synthesis process was monitored using nuclear magnetic resonance (NMR) **spectroscopy** After completion of hydrosilylation and hydrolysis reactions, proton NMR (^{1}H-NMR) and carbon NMR (^{13}C NMR) were used to monitor the reactions (Figure 5-6). The proton peaks at δ 5.2-5.4 and δ 5.9 ppm corresponding to the double bond of allyl PEG and tBA starting materials disappeared. The hydride proton peak at δ 4.8 ppm also completely disappeared due to successful hydrosilylation of PEG and tBA to the PDMS backbone producing PDMS/PEG/tBA graft copolymer. Figure 5 showed ^{1}H NMR of the final product (APGC). The carboxylic acid proton peak can be observed at i. The enlargement of peak i (δ 11 ppm) was shown in the small box. The peaks at a and f represent methylene groups. The peaks at b, c, d, e, h, and g represent methyl groups. For further confirmation ^{13}C NMR was run. In ^{13}C NMR (Figure 6), the double bond carbon peak of starting material PEG at δ 110-130 ppm was not observed after hydrosilylation. The tert-butyl CH_3 peak at δ 29.0 ppm and the tertiary carbon from acrylate at δ 85.7 ppm disappeared. The tert butanol group was hydrolyzed and the singlet carbonyl group at j (δ 160 ppm) could be seen indicating the completion of hydrolysis forming APGC with

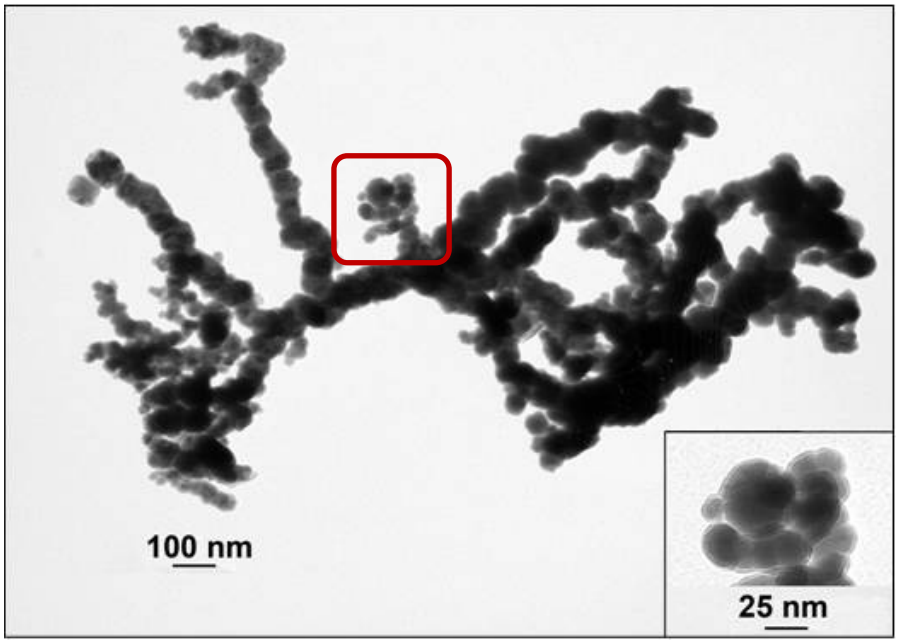

Figure 2. TEM images of bare NZVI (reproduced after Bezbaruah et al., 2009). The inset shows a zoomed in portion of the main image where the thin layer of iron oxides can be seen around the nanoparticle.

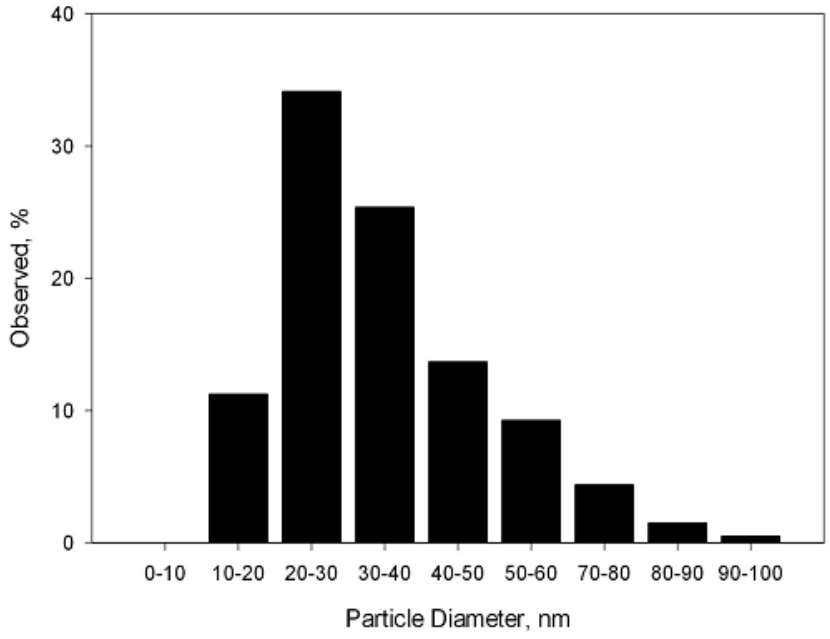

Figure 3. Particle size distribution of NZVI (n = 205) (reproduced after Bezbaruah et al., 2009)

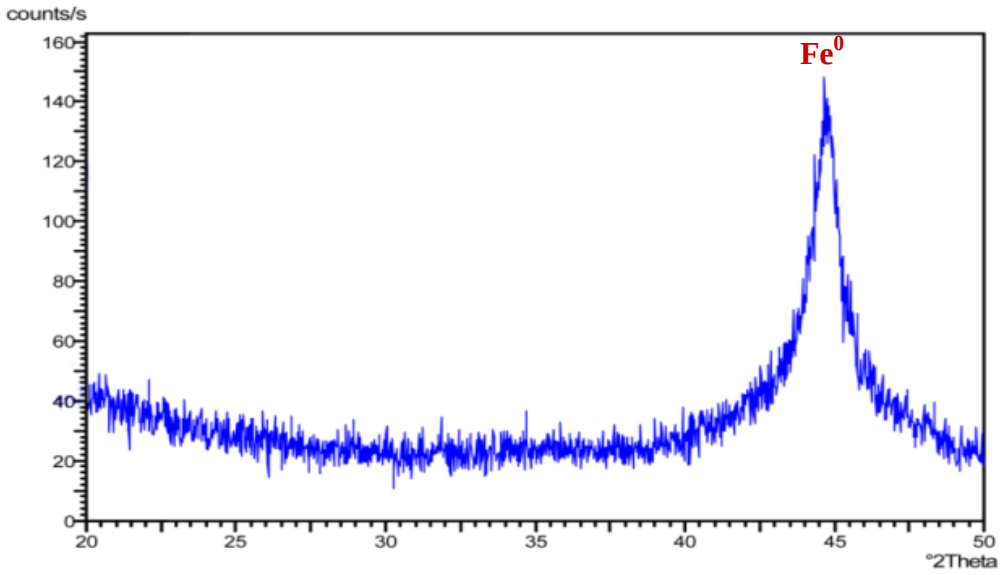

Figure 4. XRD spectrum of synthesized NZVI showed only Fe^0 (reproduced after Bezbaruah et al., 2009)

Table 2. The characteristics of the synthesized NZVI and the commercial grade MZVI

Parameter	NZVI	MZVI*
Particle size	35 nm	10 µm**
BET specific surface area	25 m^2g^{-1}	1 m^2 g^{-1}**
% Fe	84.34	99.6
% O	15.66***	0.4***

* MZVI was not used in this study but shown in this table for comparison purposes only
**Reported by Sigma-Aldrich
***The relative higher percentage of oxygen in NZVI may be to be because of it higher surface area as compared to MZVI

carboxylic acid anchoring groups. The anchoring groups were expected to attach to the NZVI surface.

Fourier transform infrared (FTIR) spectroscopy was also used to examine the polymers before and after hydrolysis (i.e., PDMS/PEG/tBA, Figure 7a and PDMS/PEG/AA, Figure 7b). The spectra showed a noticeable shift of the position of the carbonyl peak from 1732 cm^{-1} to 1712 cm^{-1}. The appearance of hydroxyl peak from 3000 cm^{-1} to 3500 cm^{-1} due to $\nu(O\text{-}H)_{COOH}$ indicates complete hydrolysis (Figure 7b) (Kataby et al., 1999). Table 3 shows the peak assignments and wave numbers for FTIR spectra of polymer before hydrolysis (PDMS/PEG/tBA), polymer after hydrolysis (PDMS/PEG/AA), and CNZVI.

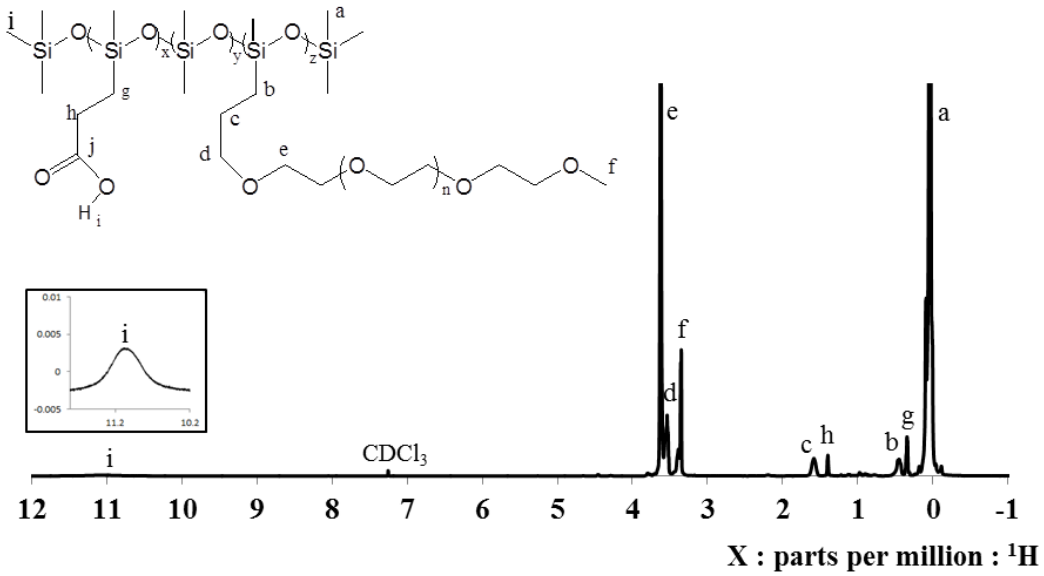

Figure 5. ^{1}H NMR of the final product (APGC). The carboxylic acid proton peak can be observed at i. The enlargement of peak i was shown in the small box. The peaks at a and f represent methylene groups. The peaks at b, c, d, e, h, and g represent methyl groups.

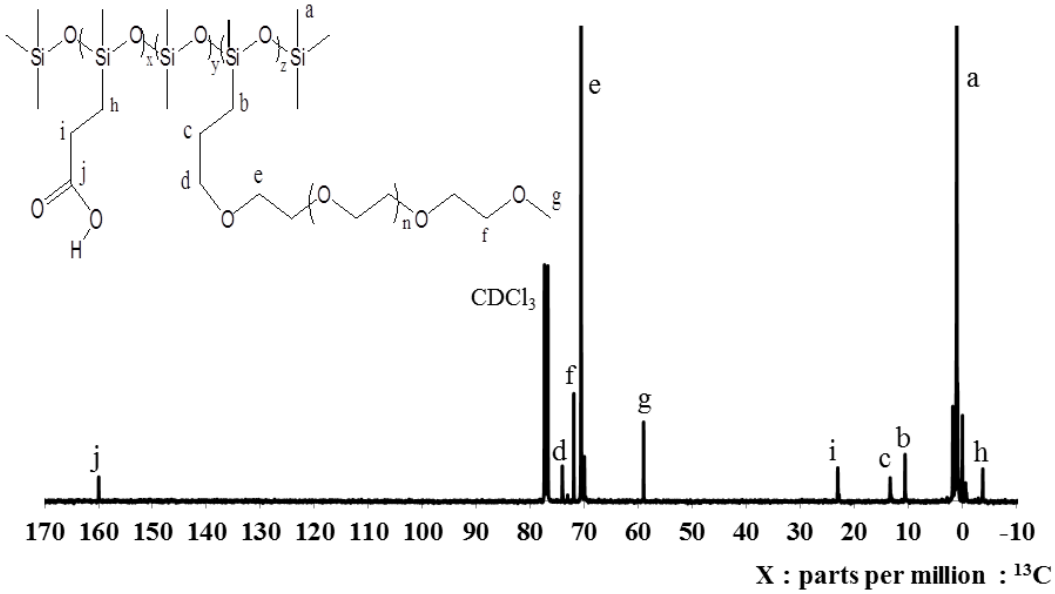

Figure 6. ^{13}C NMR spectrum of APGC (after hydrolysis). This ^{13}C NMR was done to verify the results obtained with ^{1}H NMR (Figure 5). The tert-butyl CH_3 peak at δ 29.0 ppm and the tertiary carbon from acrylate at δ 85.7 ppm disappeared. The tert butanol group was hydrolyzed and the singlet carbonyl group at j could be seen indicating the completion of hydrolysis forming APGCs with carboxylic acid anchoring groups.

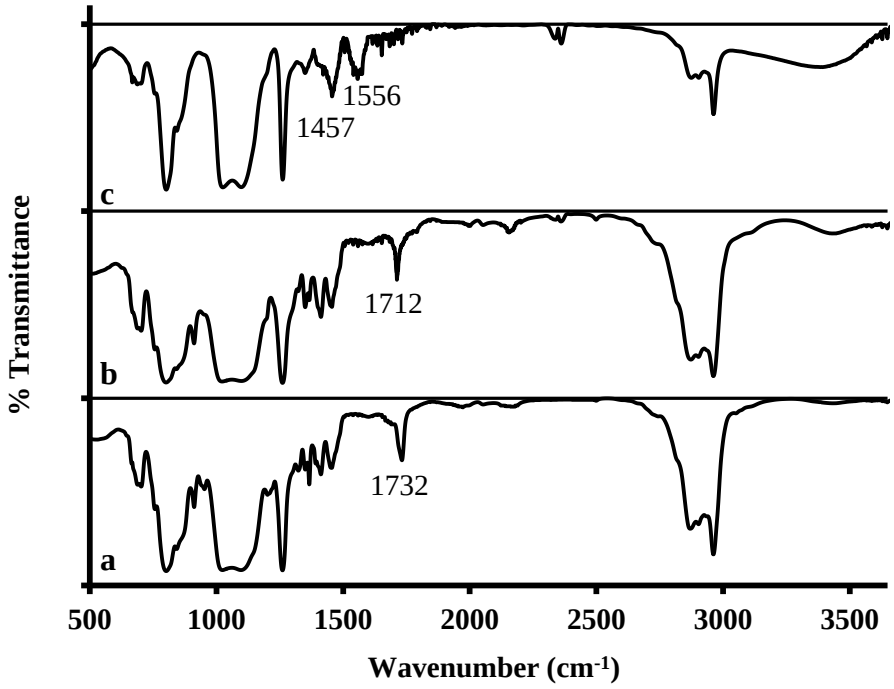

Figure 7. (a) FT-IR spectrum of APGC before hydrolysis; (b) FT-IR spectrum after hydrolysis; (c) FT-IR spectrum of CNZVI.

Table 3. Peak assignments and wave numbers for FTIR spectra of polymer before hydrolysis (PDMS/PEG/tBA), polymer after hydrolysis (PDMS/PEG/AA), and CNZVI.

Peak Assignment	PDMS/PEG/tBA (cm^{-1})	PDMS/PEG/AA (cm^{-1})	CNZVI (cm^{-1})
O-H stretch	-	3200-3500	3050-3550
-CH_2 (asymmetric)	2957	2960	2962
-CH_3 stretch	2900	2898	2879
-CH_2 (symmetric)	2861	2868	2869
C=O stretch	1732	1712	-
-COO stretch (asymmetric)	-	-	1556
-COO stretch (symmetric)	-	-	1456
C-O-C stretch	1256	-	-
$(C\text{-}O)_{COOH}$ stretch	-	1260	1261
C-O-C (broad)	1010-1093	1015-1105	1016-1085

Differential scanning calorimetry (DSC) was used to determine the influence of pendant group grafting on thermal properties (Figures 8). The PDMS starting material exhibits a glass transition temperature, T_g, at -130°C and no melting transition. After grafting PEG side chains to the PDMS, a broad melting transition over the temperature range of approximately -70°C to 0°C

was observed which was attributed to PEG side-chain crystallization. Incorporating carboxylic acid groups into the PDMS-PEG graft copolymer produced an amorphous copolymer exhibiting a single T_g at -94°C (Figure 8). The results indicate that the APGC produced was a single phase, amorphous material with a very low T_g which was expected to readily enable diffusion of groundwater contaminants to the particle surface.

CNZVI preparation

FTIR spectra of NZVI and CNZVI confirm that APGC were coated onto NZVI surface (Figure 7c). The FTIR spectra for bare NZVI did not show any significant peaks while the spectra for CNZVI showed the formation of chemical bonds (C=O stretching) between carboxylic groups and amorphous surface of NZVI. The C=O peak of carboxylic groups originally at 1712 cm^{-1} (Figure 7b) disappeared (Figure 7c), while the peaks at 1556 cm^{-1} and 1457 cm^{-1} were observed after the NZVI particles were coated with APGC. Kataby et al. (1999) observed similar peak shift while coating carboxylic acid onto amorphous iron nanoparticles.

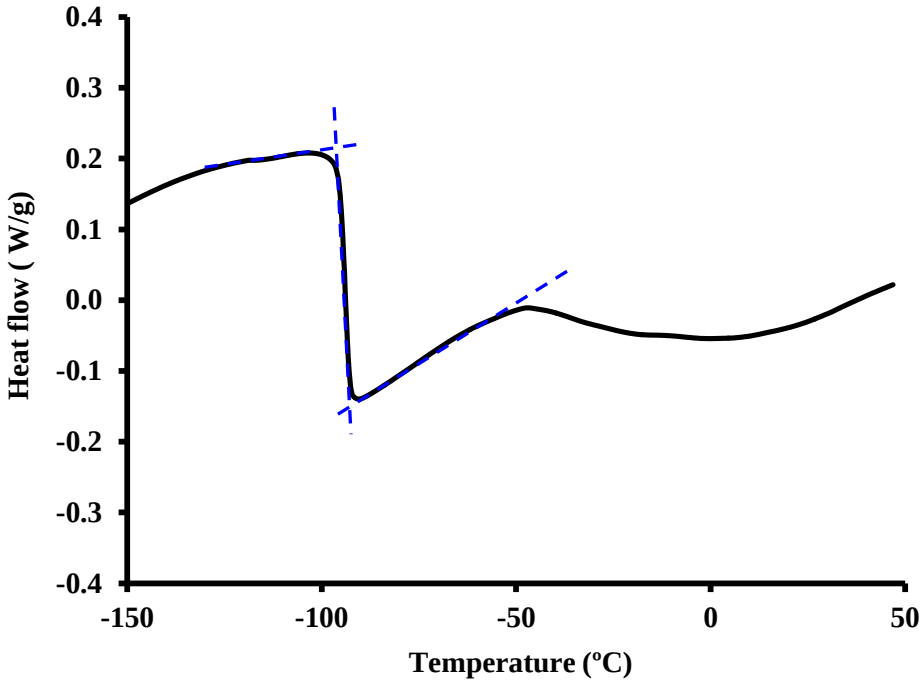

Figure 8. Differential scanning calorimetry (DSC) thermogram of APGC.

Colloidal stability studies

NZVI coated with three APGC concentrations (2, 10, and 15 g/L) were used in sedimentation studies, and the NZVI coated with 15 g/L APGC formed the most stable suspension as compared to the lower APGC concentrations and bare NZVI. White gel like precipitates were formed at APGC concentrations >15 g/L and were considered unsuitable for coating NZVI. All further analyses were conducted with CNZVI coated with 15 g/L APGC. To

determine the effect of the functional groups on sedimentation characteristics of CNZVI, the percent weight fraction of PDMS, PEG, and AA was changed systematically (Table 1). The change in PEG/AA ratio had a profound effect on colloidal stability of CNZVI. The APGC with the highest concentration of AA anchoring groups (72.5/21/6.5: PDMS/PEG/AA) provided the highest colloidal stability (Figures 9) and was used for further experimentation.

The APGC absorbed onto NZVI surface attributed to increased steric hindrance and that might have improved the colloidal stability of NZVI suspensions and can be expected to decrease adhesion to soil surfaces (Stokes and Evans, 1997). Rahme et al. (2009) used di- and tri-block copolymers poly(ethylene oxide) and poly(propylene oxide) to stabilize gold nanoparticles (~12 nm) in aqueous media, and concluded that amphiphilic nature of the polymer contributed to colloidal stability. The present copolymer coating helped steric suspension of the particles. It is worth mentioning that the sedimentation studies were conducted for all the nanoparticles (all sizes) without any presedimentation. This is in contrast to work reported by others where particles were presettled for 5-60 min to separate the larger (agglomerated) particles (Tiraferri et al., 2008; Phenrat et al., 2007).

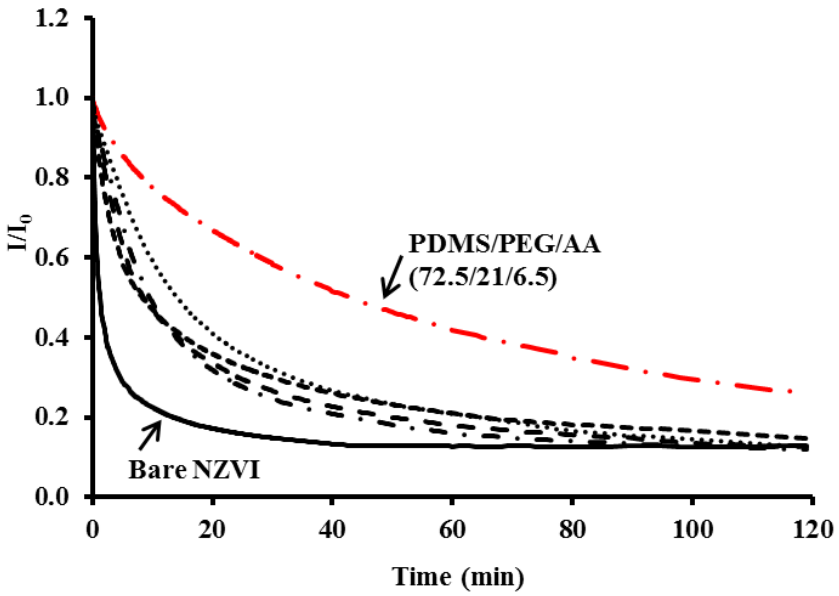

Figure 9. The APGC with the highest acrylic acid group (PDMS/PEG/AA (72.5/21/6.5)) showed the highest colloidal stability. ‒ ·: (70/25/5); ‒ ‒ ‒: (62/36/2), ——:(72.5/21/6.5), ·····: (67/29/4), ‒ ‒ : (65/32/3), ——: Bare NZVI. I = measured light intensity, I_0 = initial light intensity.

Effect of ionic strength on colloidal stability

The variations in ionic strength due to mono-valent (5 and 10 mM NaCl) and divalent cationic (5 and 10 mM $CaCl_2$) salts did not affect sedimentation characteristics of CNZVI (Figure 10). In this study there was no difference in sedimentation behavior of the CNZVI at various ionic strengths apparently because all carboxyl groups chelated to the iron leaving no

free carboxyl ion. Absence of carboxylic-carbonyl group in FTIR spectrum at 1712 cm^{-1} in CNZVI (Figure 7c) confirms that there was no unreacted/unattached carboxylic acid group left and justifies the assumption about possible complete chelation of the acid group to iron. Saleh et al. (2008) conducted column studies to investigate the effects of Na^{+} and Ca^{2+} on the mobility of surface modified NZVI in water. They found that the mobility of NZVI coated with charged surface modifiers decreased with increasing salt concentration,, and divalent cation (Ca^{2+}) had a greater effect than monovalent cation (Na^{+}) (Saleh et al., 2008). This is in contrast to the findings in this study. The triblock copolymers (analogous to the APGC designed within this research) used by Saleh et al. (2008) had a large number of charged sulfonate groups that apparently got distributed throughout an extended polymer layer on the nanoparticle surface. The surface modification of NZVI increased the negative surface potential of the particles and affected dispersibility of CNZVI under high ionic conditions. The triblock copolymer coating on the NZVI particles offered electrosteric stabilization of the particles and provided the greatest resistance to adverse effects (mobility reduction) under low salt concentration conditions but was ineffective at Ca^{2+} > 2 mM (Saleh et al., 2008). The present APGC coated NZVI particles were not affected by high Ca^{2+} concentration (10 mM) as the coated particles had no charges and their stability was steric in nature. It is expected that sticking coefficient of APGC coated NZI will be negligible and the CNZVI can be injected into the aquifer easily and a large zone of influence can be achieved.

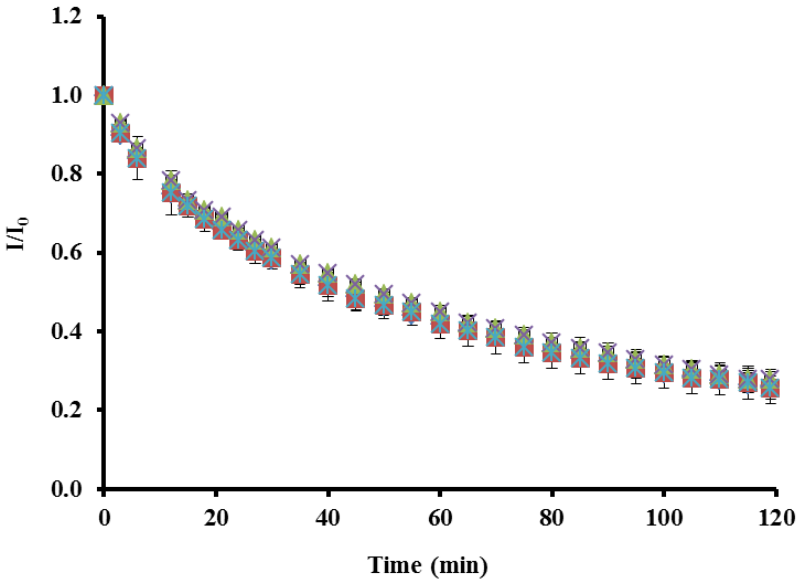

Figure 10. Sedimentation studies of CNZVI in water with different ionic strengths. The concentration of APGC used for coating was 15 mg/L and 3 g/L NZVI was used. The data points are connected with straight lines for ease of reading only and they do not represent trendlines. The vertical error bars indicate ± standard deviations. ◆ DI water, ▲ 5 mM NaCl, ■ 10 mM NaCl, × 5 mM $CaCl_2$, ✳ 10 mM $CaCl_2$.

Effect of aging on colloidal stability of CNZVI

The CNZVI particles need to have long shelf-life to be commercially viable (storage and transportability requirements). The results showed that the colloidal stability of the CNZVI remained unchanged for 12 months (two-way ANOVA, $\alpha = 0.05 <$ p-value$_{0 \text{ and } 1\text{month}} = 0.395$, p-value$_{0 \text{ and } 12 \text{ month}} = 0.245$, Figure 11).

TCE degradation studies

The results from degradation batch studies indicate effective removal of TCE by CNZVI. After 5 h, the TCE concentration decreased from the initial 30 mg/L to 5.64 mg/L (84% removal) and 2.38 mg/L (90% removal) for bare NZVI and CNZVI, respectively (Figure 12). No significant decrease of TCE was observed for either the control or the blank. A two-way ANOVA analysis of variance test on the degradation data indicated that there was a significant difference between TCE degradation by bare NZVI and CNZVI ($\alpha = 0.05 >$ p-value = 0.035). Similar results were obtained in batch studies with initial TCE concentrations of 15 and 1 mg/L (Figures 13 and 14). For 15 mg/L initial TCE concentration, removal efficiencies were 76% and 83% for NZVI and CNZVI, respectively (Figure 13). With 1 mg/L initial TCE concentration removal efficiencies were 75% and 78% for NZVI and CNZVI, respectively (Figure 14).

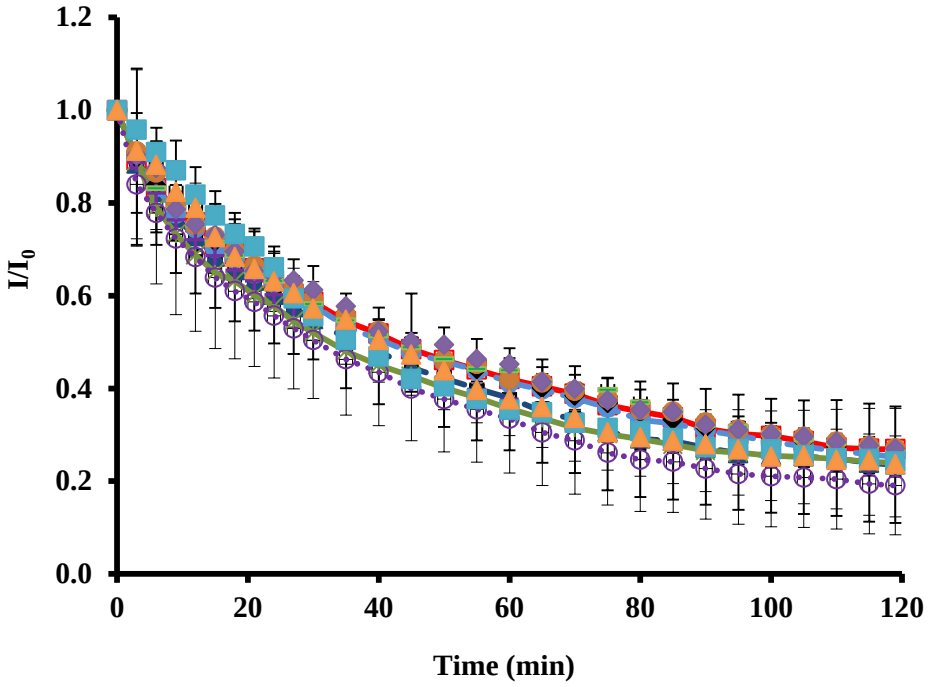

Figure 11. Sedimentation studies for CNZVI over a 12-month period for shelf-life evaluation. The data points are connected with straight lines for ease of reading only and they do not represent trendlines. The vertical error bars indicate ± standard deviations. 0 month, 1 month, 2 month, 3 month, 4 month, 5.5 month, 6 month, 7 month, 8 month, 9 month, 10 month, 11 month, and 12 month. I = measured light intensity, I_0 = initial light intensity.

The TCE degradation reaction was found to follow pseudo first-order kinetics which is common for the dehalogenation of organic compounds by NZVI (Johnson et al., 1996; Nurmi et al., 2005). The classical first-order rate reaction is expressed as in Eq. 2.

$$\frac{dC}{dt} = k_{obs} C \tag{2}$$

where

C = TCE concentration (mg/L)
k_{obs} = the observed rate constant (h^{-1})

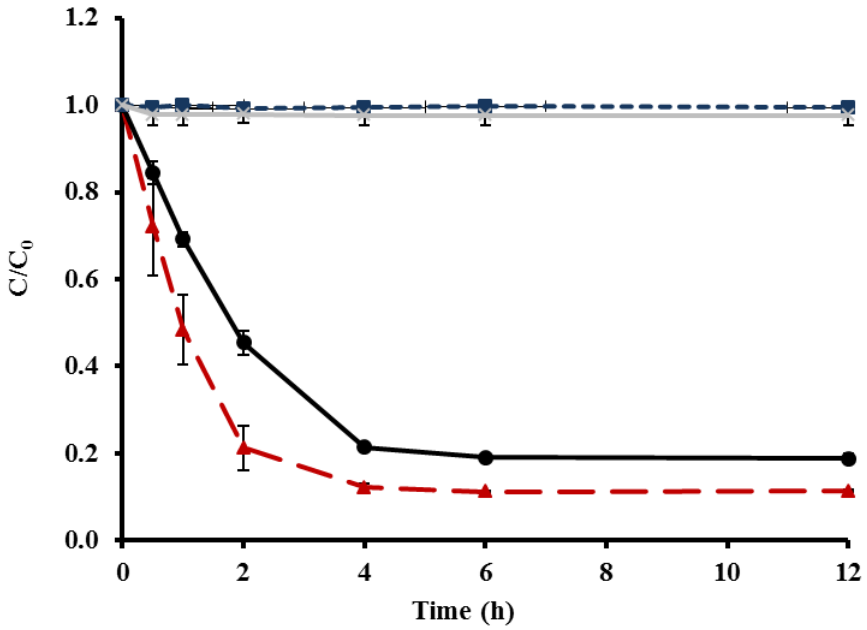

Figure 12. Dechlorination of TCE by bare NZVI and CNZVI. Initial TCE concentration = 30 mg/L. The data points are connected with straight lines for ease of reading only and they do not represent trendlines. The vertical error bars indicate ± standard deviations. CNZVI, Bare NZVI, Blank, Control.

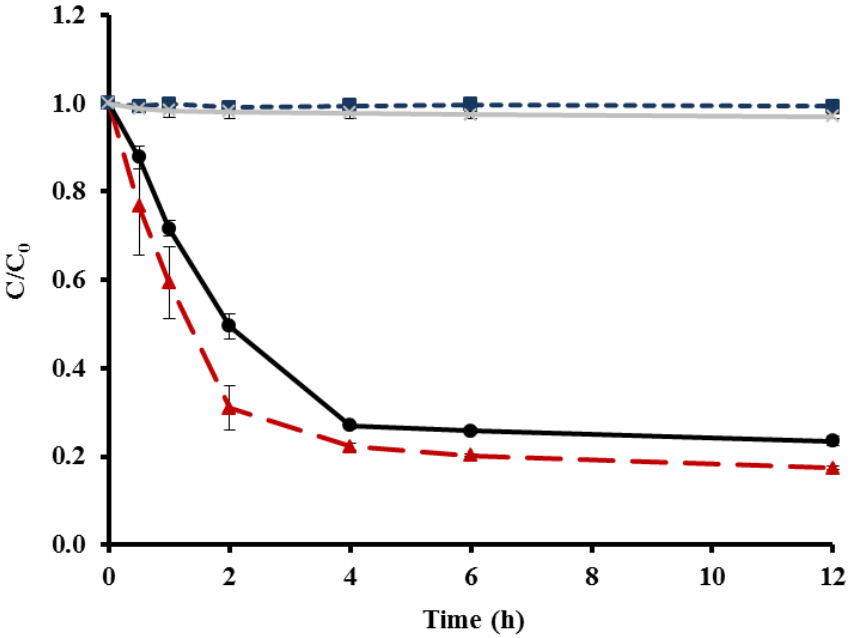

Figure 13. Dechlorination of TCE by bare NZVI and CNZVI. Initial TCE concentration = 15 mg/L. The data points are connected with straight lines for ease of reading only and they do not represent trendlines. The vertical error bars indicate ± standard deviations. CNZVI, Bare NZVI, Blank, Control.

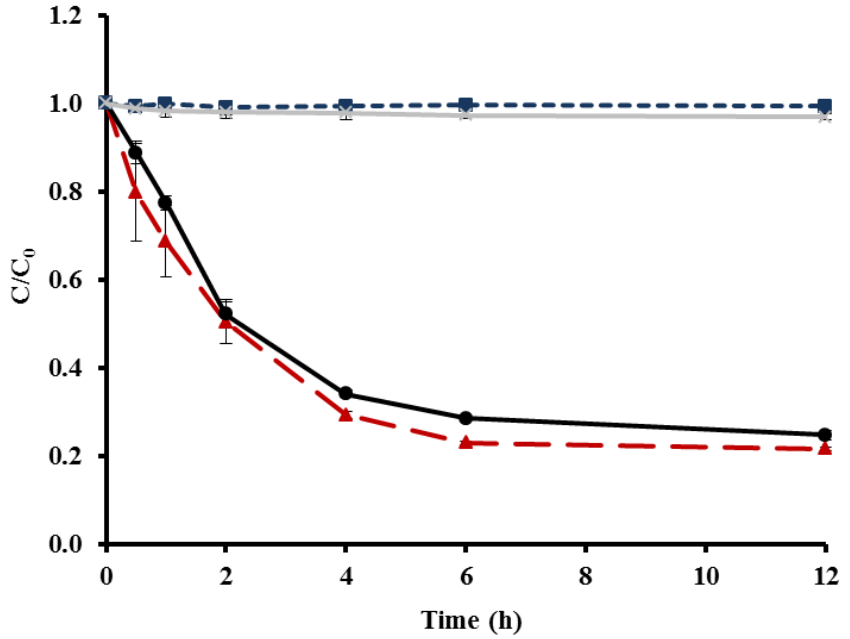

Figure 14. Dechlorination of TCE by bare NZVI and CNZVI. Initial TCE concentration = 1 mg/L. The data points are connected with straight lines for ease of reading only and they do not represent trendlines. The vertical error bars indicate ± standard deviations. CNZVI, Bare NZVI, Blank, Control.

In the case of heterogeneous reactions, such as NZVI-mediated dehalogenation, it is instructive to normalize k_{obs} with respect to (iron) surface area. It is believed that normalizing reaction rare with respect to surface area allows for more valid comparisons with different sized iron particles (Johnson et al., 1996; Nurmi et al., 2005; Thompson et al., 2010). Most researchers reported nanoscale iron reaction rate constants on a surface area normalized basis. Johnson et al. (1996) have presented the following surface area normalized first-order rate equation:

$$\frac{dC}{dt} = k_{SA}\rho_A C \tag{3}$$

where

k_{SA} = surface area normalized rate constant (L m^{-2} h^{-1})
ρ_A = iron surface area per solution volume (m^2 L^{-1})

Therefore,

$$k_{OBS} = k_{SA}\,\rho_A \tag{4}$$

Surface normalized reaction rate constants, k_{SA}, for TCE degradation ranged from 0.007-0.016 $Lm^{-2}h^{-1}$ to 0.008-0.024 $Lm^{-2}h^{-1}$ for bare NZVI and CNZVI (Table 4).

The results from the present study indicate no adverse effect of the polymer coating on NZVI reactively, rather the reactivity significantly increased when particles were coated with APGC. This is in contrast to findings by Lowry's research group (Phenrat et al., 2009). Lowry's group found that NZVI surface modification with poly(styrene sulfonate), carboxymethyl cellulose, and polyaspartate enhanced colloidal stability and subsurface mobility of the particles but the reactivity had gone down nonlinearly with the amount of surface modifier used. Blocking of reactive surface sites on the particles and partitioning of TCE to the surface modifiers was suggested as the possible reasons for the decrease in reactivity up to 24 times as compared bare NZVI (Phenrat et al., 2009). There was no loss of reactivity of NZVI due to coating in the present study possibly because of the nature of the constituent groups of the APGC developed. PDMS used in the APGC is known to permeate organic contaminants without partitioning (Stokes, 1997). Statistical analysis of TCE degradation data indicated that there was no significant difference (two-way ANOVA, $\alpha = 0.05 <$ p-value = 0.245) between the blank (only TCE) and the control (APGC and TCE) validating the point that there was no partitioning of TCE into the copolymer.

Effect of aging on TCE degradation by CNZVI

The CNZVI particles need to have long shelf-life to be commercially viable (storage and transportability requirements). The results showed that the TCE degradation rate remained more or less constant (k_{SA} = 0.023 – 0.024 $Lm^{-2}h^{-1}$) over a six-month period ($\alpha = 0.05 <$ p-$value_{0and1month}$= 0.224, p-$value_{0and6month}$= 0.103, Figure 15). Having such a long shelf-life will make CNZVI more attractive to remediation practitioners. It is worth mentioning that shelf-life

of NZVI evaluated using sedimentation behavior as the criterion was found to be 12 months (See Effect of aging on colloidal stability of CNZVI).

Table 4. TCE degradation reaction rate constants with bare NZVI and CNZVI.

	Observed Reaction Rate K_{obs} (h^{-1})	Surface Normalized Reaction Rate k_{SA} ($L\ m^{-2}\ h^{-1}$)	Correlation Coefficient R^2
Initial TCE = 30 mg/L			
Bare NZVI	0.389	0.016	0.999
CNZVI	0.90	0.024	0.987
Initial TCE = 15 mg/L			
Bare NZVI	0.332	0.008	0.997
CNZVI	0.424	0.011	0.902
Initial TCE = 1 mg/L			
Bare NZVI	0.278	0.007	0.985
CNZVI	0.317	0.008	0.986

Average NZVI particle diameter = 35 nm; NZVI surface area = 25 m^2g^{-1}; NZVI surface area concentration in the test solution (ρ_A) = 37.5 m^2L^{-1}

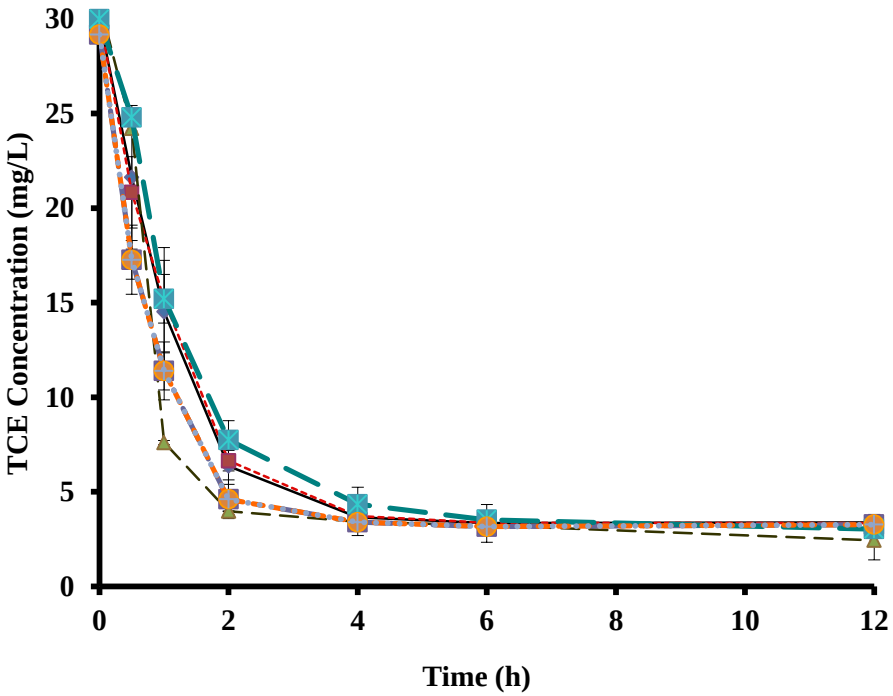

Figure 15. TCE degradation studies using CNZVI over a 6-month period (shelf-life evaluation). The data points are connected with straight lines for ease of reading only and they do not represent trendlines. The vertical error bars indicate ± standard deviations. 0 month, 1 month, 2 months, 3 months, 4 months, 5 months, 6 months.

As(V) removal batch studies

As(V) adsorption kinetics were investigated in batch with a constant NZVI/CNZVI mass (0.75 g NZVI/L) and varying As(V) initial concentrations (1, 5, and 10 mg/L; Figures 16-18). The results showed higher As(V) removal by CNZVI than bare NZVI in both aerobic and anaerobic conditions. Under aerobic conditions, 99.6 to 100% As(V) was removed by CNZVI in 2 hwhile bare NZVI removed 84.5 to 95.7% during the same 2 h period. Sun et al. (2006) also found that both arsenate and arsenite compounds could be removed efficiently by using ZVI under aerobic and relative anaerobic conditions. While aerobic conditions were favorable for As(V) removal, As(III) could be removed more rapidly than As(V) under anaerobic condition (Sun et al., 2006). Tanboonchuy et al. (2011) made similar observations about As(V) removal under oxygen depleted conditions. They recorded 99% removal of As(V) within 7 min of reaction with NZVI under oxic conditions, while only 76% removal was observed under deoxygenated environment (Tanboonchuy et al., 2011). Water oxidizes iron (Fe^0) to Fe^{2+} in anaerobic (Eq. 5) and dissolved oxygen also participates in the iron oxidation process under aerobic conditions (Eq. 6) (Tanboonchuy et al., 2011).

$$Fe^0 + 2H_2O \leftrightarrow Fe^{2+} + H_2 + 2OH^- \quad (5)$$

$$2Fe^0 + 2H_2O + O_2 \leftrightarrow 2Fe^{2+} + 4OH^- \quad (6)$$

Arsenic removal can be enhanced in the presence of oxygen because arsenic can form inner- and/or outer-sphere complexes with the oxygen-induced iron corrosion products such as iron (hydr)oxides (Zhang et al., 2004; Bang et al., 2005; Mayo et al., 2007). The presence of DO in water enhances the rate of iron corrosion and consequently improves arsenic removal by NZVI (Tanboonchuy et al., 2011).

The removal of As(V) by both CNZVI and bare NZVI was found to follow pseudo-first-order reaction kinetics (Table 5). The surface normalized reduction rate constants (from Eq. 4) for As(V) removal by CNZVI under aerobic conditions for all initial As(V) concentrations (1, 5, and 10 mg/L) were determined to be greater (k_{SA} = 0.308-0.376 Lm^{-2} h^{-1}) as compared to those under anaerobic conditions (k_{SA} = 0.152-0.258 Lm^{-2} h^{-1}). The same observation was made for As(V) removal by bare NZVI under aerobic (k_{SA} = 0.115-0.219 Lm^{-2} h^{-1}) and anaerobic conditions (k_{SA} = 0.102-0.193 Lm^{-2} h^{-1}). Kanel et al. (2006) showed 100% removal of As(V) using bare NZVI and the reaction was found to follow the pseudo-first-order adsorption kinetics with observed reaction constants (k_{obs}) of 1.2 to 42.6 h^{-1} and surface area normalized rate constants (k_{SA}) of 0.9 to 1.74 Lm^2 h^{-1}.

Table 5. Arsenic removal rate constants with bare NZVI and CNZVI.

	Observed Reaction Rate k_{obs} (h^{-1})	Surface Normalized Reaction Rate k_{SA} ($L\ m^{-2}\ h^{-1}$)	Correlation Coefficient R^2
Initial As(V) = 10 mg/L			
Bare NZVI (aerobic)	2.168	0.115	0.912
Bare NZVI (anaerobic)	1.930	0.102	0.925
CNZVI (aerobic)	5.790	0.308	0.981
CNZVI (anaerobic)	2.857	0.152	0.847
Initial As(V) = 5 mg/L			
Bare NZVI (aerobic)	2.916	0.155	0.907
Bare NZVI (anaerobic)	2.798	0.149	0.930
CNZVI (aerobic)	5.900	0.315	0.893
CNZVI (anaerobic)	3.777	0.201	0.953
Initial As(V) = 1 mg/L			
Bare NZVI (aerobic)	4.111	0.219	0.962
Bare NZVI (anaerobic)	3.635	0.193	0.965
CNZVI (aerobic)	7.047	0.376	0.986
CNZVI (anaerobic)	4.855	0.258	0.917

Average NZVI particle diameter = 35 nm; NZVI surface area = 25 m^2g^{-1}; NZVI surface area concentration in test solution (ρ_A) = 18.75 m^2L^{-1}

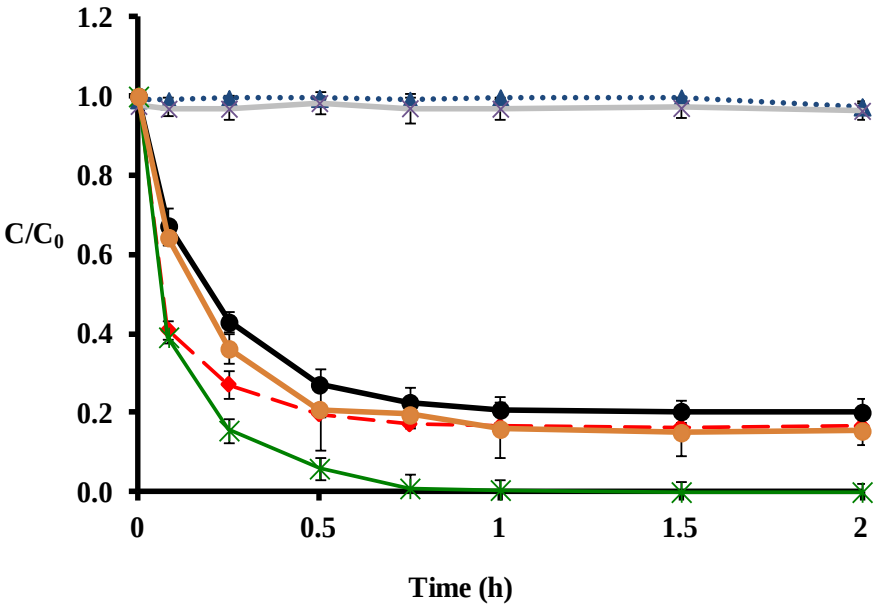

Figure 16. As(V) removal over time (initial As(V) concentration is 10 mg/L). C/C_0 is the normalized concentration of As(V). The data points are connected with straight lines for ease of reading only and they do not represent trendlines. The vertical error bars indicate ± standard deviations. CNZVI (anaerobic), Bare NZVI (anaerobic), Bare NZVI (aerobic), CNZVI (aerobic), Blank, Control.

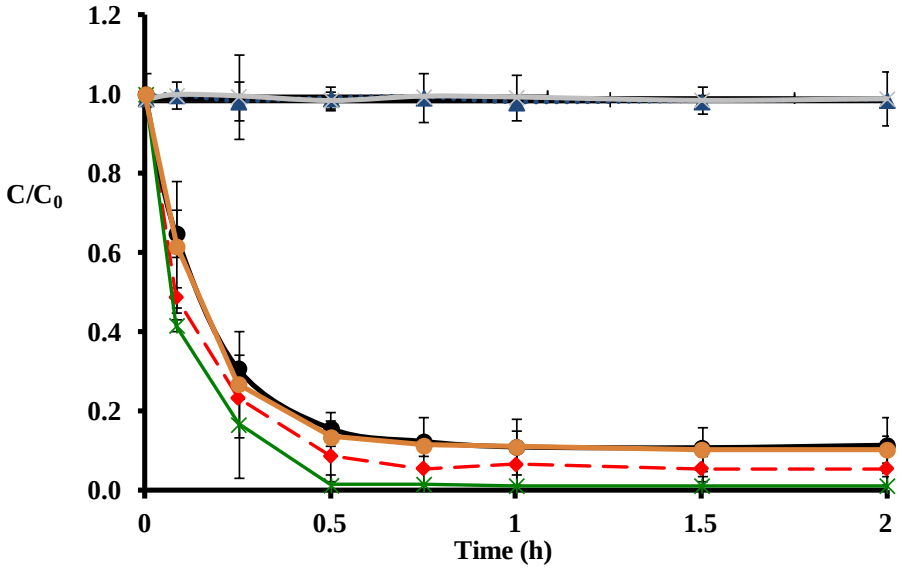

Figure 17. As(V) removal over time (initial As(V) concentration is 5 mg/L). C/C_0 is the normalized concentration of As(V). The data points are connected with straight lines for ease of reading only and they do not represent trendlines. The vertical error bars indicate ± standard deviations. CNZVI (anaerobic), Bare NZVI (anaerobic), Bare NZVI (aerobic), CNZVI (aerobic), Blank, Control.

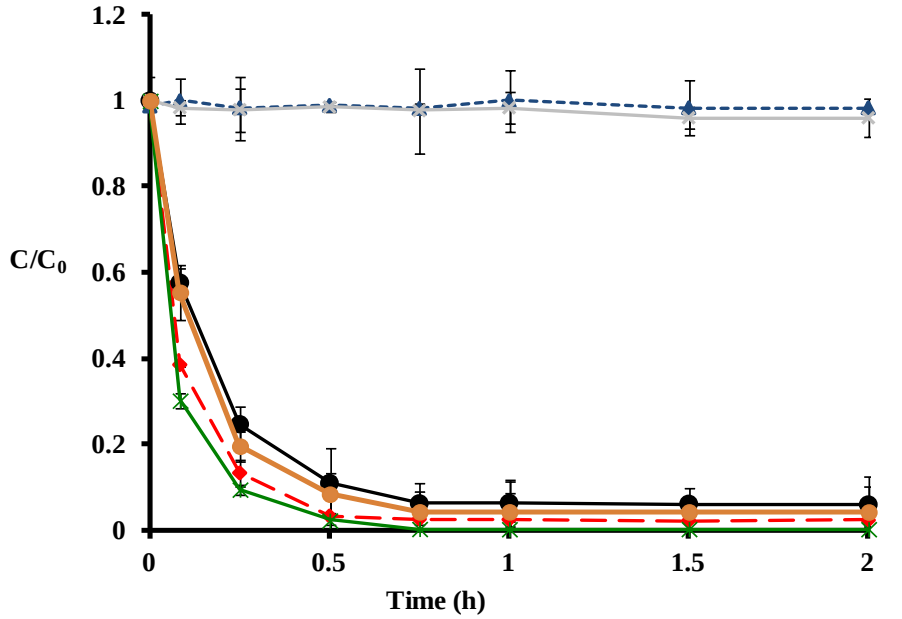

Figure 18. As(V) removal over time (initial As(V) concentration is 1 mg/L). C/C_0 is the normalized concentration of As(V). The data points are connected with straight lines for ease of reading only and they do not represent trendlines. The vertical error bars indicate ± standard deviations. CNZVI (anaerobic), Bare NZVI (anaerobic), Bare NZVI (aerobic), CNZVI (aerobic), Blank, Control.

Effect of ionic strength on As(V) removal

Batch experiments were conducted to investigate the efficiency of CNZVI in As(V) removal in ionic solutions. The results showed minimal adverse effect of ionic strength. There was only ~4% decrease in removal efficiency in the presence of 10 mM NaCl and ~8% decrease when 10 mM $CaCl_2$ was used (Figure 19). The 4-8% decrease in removal efficiency was observed when compared to removal efficiency without $CaCl_2$/NaCl. Biterna et al. (2010) found decrease in arsenic removal (~7%) in the presence of chloride. The inhibiting effect of chloride has also been reported in the removal of perchlorate by ZVI and was attributed to the competition for sorption sites on ZVI surface (Moore and Young, 2005).

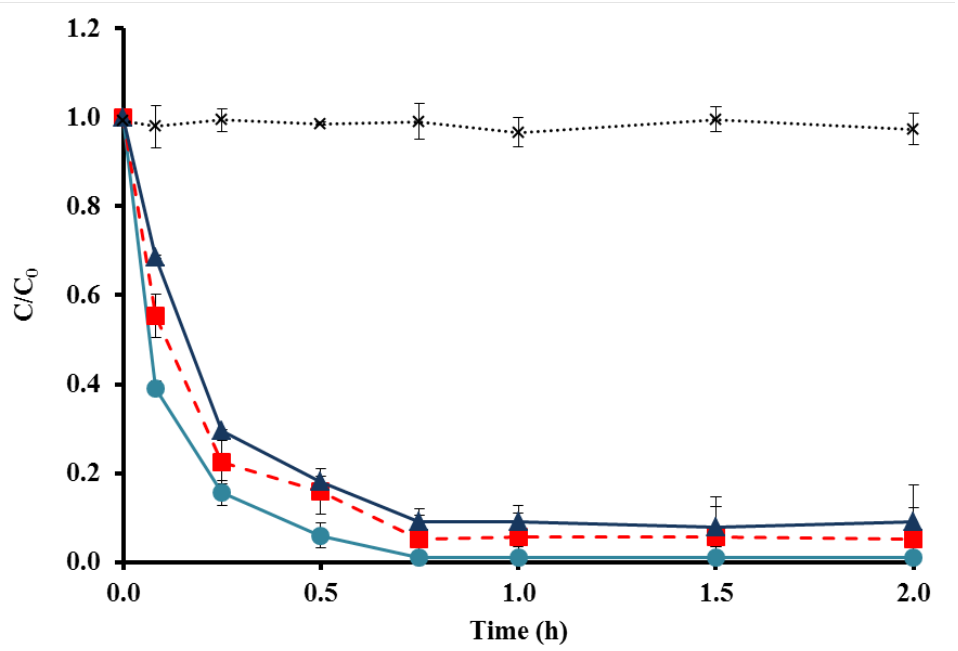

Figure 19. Effects of ionic strength on arsenic removal by CNZVI under aerobic conditions. C/C_0 is the normalized concentration of As(V). The data points are connected with straight lines for ease of reading only and they do not represent trendlines. The vertical error bars indicate ± standard deviations. CNZVI+As(V); CNZVI+As(V)+10mM NaCl); CNZVI+As(V)+10mM $CaCl_2$; Blank.

CONCLUSIONS

This research targeted at improving the reactivity of nanoscale zero-valent iron (NZVI) particles for groundwater contaminant removal. The nanoparticles tend to agglomerate due to magnetic and van der Waals forces. Agglomerated particles are larger in size and have reduced specific reactive surface area. Zero-valent iron reactions are known to be surface area mediated and, hence, the prevention of agglomeration of the particles was expected to improve NZVI reactivity. The key to improving NZVI reactivity was to increase dispersibility of the nanoparticles. A novel ampliphilic polysiloxane graft copolymer (APGC) was used to overcome

the NZVI agglomeration problems. APGC was synthesized and coated onto NZVI particles to enhance their dispersibility (colloidal stability). Treatability studies were conducted for trichloroethylene (TCE) and arsenic [As (V)]. Coating the NZVI particles with APGC was found to enhance their colloidal stability. It was also found that the colloidal stability of the APGC coated NZVI remained effectively unchanged up to 12 months. Moreover, different concentrations (0-10 mM) of NaCl and $CaCl_2$ representing groundwater ionic strengths had no impact on sedimentation behavior of the APGC coated NZVI.

The results from TCE degradation batch studies with APGC coated NZVI (CNZVI) indicated effective removal of TCE. TCE degradation was found to be better with CNZVI compared to bare NZVI. The TCE concentration decreased from the initial 30 mg/L to 5.64 mg/L (84% removal) and 2.38 mg/L (90% removal) for bare NZVI and CNZVI, respectively. The surface normalized degradation rate constants, k_{SA} ($Lm^{-2}\ h^{-1}$), for TCE removal by CNZVI and bare NZVI ranged from 0.008-0.024 to 0.070-0.016, respectively when initial TCE concentration ranged from 1 to 30 mg/L. It was also found that TCE degradation capacity of the APGC coated NZVI remain effectively unchanged up to 6 months of storage.

As(V) removal using CNZVI was tried and the results showed higher As(V) removal using CNZVI than bare NZVI under both aerobic and anaerobic conditions. Under anaerobic conditions, the As(V) removal by CNZVI and bare NZVI ranged from 83.4% to 90.6% and 79% to 94% in 2 h, respectively. The surface normalized reaction rate constants of As(V) by CNZVI under aerobic conditions for all initial As(V) concentrations (1, 5, and 10 mg/L) were determined to be greater (k_{SA} = 0.308-0.376 $Lm^{-2}\ h^{-1}$) compared to the rate constants found under anaerobic conditions (k_{SA} = 0.152-0.258 $Lm^{-2}\ h^{-1}$), and bare NZVI under both aerobic (k_{SA} = 0.115-0.219 $Lm^{-2}\ h^{-1}$) and anaerobic conditions (k_{SA} = 0.102-0.193 $Lm^{-2}\ h^{-1}$). The ionic strength (NaCl and $CaCl_2$) showed minimal (4-8%) inhibiting effects on arsenic removal.

With the observed improvement in dispersibility and treatability by NZVI when coated with APGC, it is safe to claim that CNZVI has potential for groundwater remediation applications. The long shelf-life (6-12 months) achieved for CNZVI is expected to make it a commercially viable product. The new copolymer can possibly be used for other NPs for environmental and other applications.

REFERENCES

Almeelbi, T., Bezbaruah, A.N. (2012) Aqueous phosphate removal using nanoscale zero-valent iron, *J. Nanopart. Res*, 14, 1-14.

Bang, S.; Johnson, M.D.; Korfiatis, G.P.; Meng, X. (2005) Chemical reactions between arsenic and zero-valent iron in water. *Water Res.*, 39, 763-770.

Berg, M.; Tran, H.C.; Nguyen, T.C.; Pham, H.V.; Schertenleib, R.; Giger, W. (2001) Arsenic contamination of groundwater and drinking water in Vietnam: A Human health threat. *Envi. Sci. Technol*., 35, 2621- 2626.

.

Bezbaruah, A.N.; Krajangpan, S.; Chisholm, B.J.; Khan, E.; Bermudez, J.J.E. (2009) Entrapment of iron nanoparticles in calcium alginate beads for groundwater remediation applications. *J. Hazard. Mater*., 166, 1339-1343.

Bezbaruah, A., Chisholm, B., Krajangpan, S. (2011) Polymeric Delivery Vehicle for Nanoparticles. Nationalized PCT Patent, 2011/0042,325.

Bezbaruah, A.N.; Shanbhougue, S.S.; Simsek, S.; Khan, E. (2011) Encapsulation of iron nanoparticles in alginate biopolymer for trichloroethylene remediation. *J. Nanopart. Res.*, 13, 6673-6681.

Biterna, M.; Arditsoglou, A.; Tsikouras, E.; Voutsa, D. (2007) Arsenate removal by zero valent iron: Batch and column tests. *J. Hazard. Mater*., 149, 548-552.

Cao, J.; Li, X.; Tavakoli, J.; Zhang, W.-X. (2008) Temperature programmed reduction for measurement of oxygen content in nanoscale zero-valent iron. *Environ. Sci. Technol.*, 42, 3780-3785.

Chen, S.S.; Hsu, H.-D.; Li, C.-W. (2004) A new method to produce nanoscale iron for nitrate removal. *J. Nanopart. Res.*, 6, 639-647.

Cheng, R.; Wang, J.-L.; Zhang, W.-X. (2007) Comparison of reductive dechlorination of *p*-chlorophenol using Fe-0 and nanosized Fe-0. *J. Hazard. Mater.*, 144, 334–339.

Ellis, P.A.; M.O. Rivett. (2007) Assessing the impact of VOC-contaminated groundwater on surface water at the city scale. *J. Contam. Hydrol.*, 91, 107-127.

Feitz, A.J.; Joo, S.H.; Guan, J.; Sun, Q.; Sedlak, D.L.; Waite, T.D. (2005) Oxidative transformation of contaminants using colloidal zero-valent iron. *Colloid Surface A*, 265, 88-94.

Hussam. A.; Munir, A.K.M. (2007) A simple and effective arsenic filter based on composite iron matrix: Development and deployment studies for groundwater of Bangladesh. *J. Environ. Sci. Heal. A*, 42, 1869–1878.

Johnson, T.L.; Scherer, M.M.; Tratnyek, P.G. (1996) Kinetics of halogenated organic compound degradation by iron metal. *Environ. Sci. Technol*., 30, 2634-2640.

Joo, S.H.; Zhao, D. (2008) Destruction of lindane and atrazine using stabilized iron nanoparticles under aerobic and anaerobic conditions: effects of catalyst and stabilizer. *Chemosphere*, 70, 418-425.

Kanel, S.R.; Manning, B.; Chatlet, L.; Choi, H. (2005) Removal of arsenic (III) from groundwater by nanoscale zero-valent iron. *Environ. Sci. Technol.*, 39, 1291-1298.

Kanel, S.R.; Greneche, J.M.; Heechul, C. (2006) Arsenic (V) removal from groundwater using nano scale zero-valent iron as a colloidal reactive barrier material. *Environ. Sci. Technol.*, 40, 2045-2050.

Kataby, G.; Cojocaru, M.; Prozorov, R.; Gedanken, A. (1999) Coating carboxylic acids on amorphous iron nanoparticles. *Langmuir,* 15, 1703-1708

Katsenovich Y.P.; Miralles-Wilhelm, F.R. (2009) Evaluation of nanoscale zerovalent iron particles for trichloroethene degradation in clayey soils, *Sci. Total Environ.*, 407, 4986–4993.

Klimkova, S.; Cernik. M.; Lacinova, L.; Filip, J.; Jancik, D.; Zboril, R. (2011) Zero-valent iron nanoparticles in treatment of acid mine water from in situ uranium leaching. *Chemosphere,* 82, 1178–1184.

Krajangpan, Kalita, H., B. J. Chisholm, B.J., Bezbaruah, A.N. (2012) Iron nanoparticles coated with amphiphilic polysiloxane graft copolymers: Dispersibility and contaminant treatability. *Environ. Sci. Technol.*, 46, 10130-10136.

Krajangpan, S.; Chisholm, B.J.; Kalita, H.; and Bezbaruah, A.N. (2009) Challenges in groundwater remediation with iron nanoparticles: Enhancement colloidal stability (Chapter 8) in T. Zhang, R. Surampalli; K. Lai, Z. Hu, R. Tyagi, and I. Lo, Eds, Nanotechnologies for Water Environment Applications. Reston, V A: Environmental and Water Resources Institute/American Society for Civil Engineers, pp. 191-212.

Krajangpan, S.; Jarabek, L.; Jepperson, J.; Chisholm, B.; Bezbaruah, A. (2008) Polymer modified iron nanoparticles for environmental remediation. *Polymer Preprint,* 49, 921-922.

Li, L.; Fan, M.; Brown, R.C.; Van Leeuwen, J H.; Wang, J.; Wang, W.; Song, Y.; Zhang, Z. (2006) Synthesis, properties, and environmental applications of nanoscale iron-based materials: A review. *Crit. Rev. Env. Sci. Tec.*, 36, 405-431.

Lisabeth, L.D.; Hyeong, A.J.; Chen, J.J.; Shawnita, S.J.; Burke, J.F.; Meliker, J.R. (2010) Arsenic in drinking water and stroke hospitalizations in Michigan. *Stroke,* 41, 2499-2504.

Liu, Y.Q.; Lowry, G.V. (2006) Effect of particle age (Fe-o content) and solution pH on NZVI reactivity: H-2 evolution and TCE dechlorination. *Environ. Sci. Technol*., 40, 6085-6090.

Lui, Y.; Lowry, G.V. (2006) Effect of particle age (Fe^0 content) and solution pH on NZVI reactivity: H_2 evolution and TCE dechlorination. *Environ. Sci. Technol.,* 40, 6085-6090.

Martin, J.E.; Herzing, A.A.; Yan, W.L.; Li, X.Q.; Koel, B.E.; Kiely, C.J.; Zhang, W.X. (2008) Determination of the oxide layer thickness in core-shell zerovalent iron nanoparticles. *Langmuir,* 24, 4329-4334.

Matheson, L.; Tratnyek, P. (1994) Reductive dehalogenation of chlorinated methanes by iron metal. *Environ. Sci. Technol*., 28, 2045-2053.

Mayo, J.T.; Yavuz, C.; Yean, S.; Cong, L.; Shipley, H.; Yu, W.; Falkner, J.; Kan, A.; Tomson, M.; Colvin V.L. (2007) The effect of nanocrystalline magnetite size on arsenic removal. *Sci. Technol. Adv. Mat.,* 8, 71-75.

Moore, A.M.; Young, T.M., (2005) Chloride interactions with ironsurfaces: implications for perchlorate and nitrate remediationusing permeable reactive barriers. *J. Environ. Eng.*, 131, 924–933.

Nurmi, J.T.; Tratnyek, P.G.; Sarathy, V.; Baer, D.R.; Amonette, J.E.; Pecher, K.; Wang, C.; Linehan, J.C.; Matson, D.W.; Penn, R.L.; Driessen, M.D. (2005) Characterization and properties of metallic iron nanoparticles: spectroscopy, electrochemistry, and kinetics. *Environ. Sci. Technol*., 39, 1221-1230.

Pant, P.; Pant, S. (2010) A review: Advances in microbial remediation of trichloroethylene (TCE). *J. Environ. Sci.-China*, 22, 116-126.

Phenrat, T.; Liu, Y.; Tilton, R. D.; Lowry, G. V. (2009) Adsorbed polyelectrolyte coatings decrease Fe^0 nanoparticle reactivity with TCE in water: conceptual model and mechanism. *Environ. Sci. Technol.,* 43, 1507-1514.

Phenrat, T.; Long, T. C.; Lowry, G.V.; Veronesi, B. (2009) Partial Oxidation ("Aging") and Surface Modification Decrease the Toxicity of Nanosized Zerovalent Iron. *Environ. Sci. Technol.,* 43, 195-200.

Phenrat, T.; Saleh, N.; Sirk, K.; Tilton, R.D.; Lowry, G.V. (2007) Aggregation and sedimentation of aqueous nanoscale zerovalent iron dispersions. *Environ. Sci. Technol*., 41, 284-290.

Quinn, J.; Geiger, C.; Clausen, C.; Brooks, K.; Coon, C.; O'Hara, S.; Krug, T.; Major, D.; Yoon, W.S.; Gavaskar, A.; Holdsworth, T. (2005) Field demonstration of DNAPL dehalogenation using emulsified zero-valent iron. *Environ Sci Technol.,* 39, 1309–1318.

Rahme, K.; Vicendo, P.; Ayela, C.; Gaillard, C.; Payre, B.; Mingotaud, C.; Gauffre, F. (2009) A simple protocol to stabilize gold nanoparticles using amphiphilic block copolymers: stability studies and viable cellular uptake. *Chem. Eur. J.*, 15, 11151-11159.

Sabourault, N.; Mignani, G.; Wagner, A.; Mioskowski, C. Platinum oxide (PtO_2): a potent hydrosilylation catalyst. *Org. Lett.* 2002, 4, 2117-2119.

Saleh, N.; Kim, H.-J.; Phenrat, T.; Matyjaszewski, K.; Tilton, R.D.; Lowry, G.V. (2008) Ionic strength and composition affect the mobility of surface-modified Fe^0 nanoparticles in water-saturated sand columns. *Environ. Sci. Technol.,* 42, 3349-3355.

Saleh, N.; Sirk, K.; Liu, Y.; Phenrat, T.; Dufour, B.; Matyjaszewski, K.; Tilton, R. D.; Lowry, G. V. (2007) Surface modifications enhance nanoiron transport and NAPL targeting in saturated porous media. *Environ. Eng. Sci.*, 24, 45-57.

Schlicker, O.; Ebert, M.; Firth, M.; Weidner, M.; Wust, W.; Dahmke, A. (2003) Degradation of TCE with iron: the role of competing chromate and nitrate reduction. *Ground Water*, 38, 403–409.

Sohn, K.; Kang, S.W.; Ahn, S.; Woo, M.; Yang, S.K. (2006) Fe(0) nanoparticles for nitrate reduction: stability, reactivity, and transformation. *Environ. Sci. Technol*., 40, 5514-5519.

Stokes, R. J.; Evans, D. F. (1997) *Fundamentals of interfacial engineering*, Wiley-VCN: Canada.

Sun, H.; Wang, L.; Zhang, R.; Sui, J.; Xu, G. (2006) Treatment of groundwater polluted by arsenic compounds by zero valent iron. *J. Hazard. Mater. B*, 129, 297–303.

Tanboobchuy, V.; Hsu, J.C.; Grisdanurak, N.; Liao, C.H. (2011) Impact of selected solution factors on arsenate and arsenite removal by nano ironparticles. *Environ. Sci. Pollut. R.*, 18, 857-864.

Thompson, J.M.; Chisholm, B.J.; Bezbaruah, A.N. (2010) Reductive dechlorination of chloroacetanilide herbicide (alachlor) using zero-valent iron nanoparticles. *Environ. Eng. Sci.*, 27, 227-232.

Tiraferri, A.; Chen, K.; Sethi, R.; Elimelech, M. (2008) Reduce aggregation and sedimentation of zero-valent iron nanoparticles in the presence of guar gum. *J. Colloid Interface Sci.*, 324, 71-19.

Tsai, T.T.; Kao, C.M.; Wang, J.Y. (2011) Remediation of TCE-contaminated groundwater using acid/BOF slag enhanced chemical oxidation. *Chemosphere*., 83, 687-692.

Wu, C.; Schaum, J. (2000) Exposure assessment of trichloroethylene. *Environ. Health Persp.*, 108, 359-363.

Xi, Y.; Mallavarapu, M.; Naidu, R. (2010) Reduction and adsorption of Pb^{2+} in aqueous solution by nano-zero-valent iron—A SEM, TEM and XPS study. *Mater. Res. Bull.*, 45, 1361–1367.

Zhang, W.; Singh, P.; Paling, E.; Delides, S. (2004) Arsenic removal from contaminated water by natural iron ores. *Miner. Eng.*,17, 517-524.

Zhang, X.; Lin, Y.-M.; Shan, X.-Q.; Chen, Z.-L. (2010) Degradation of 2,4,6-trinitrotoluene (TNT) from explosive wastewater using nanoscale zero-valent iron. *Chem. Eng. J.*, 158, 566–570.